Magnetic properties and giant magnetoresistance in meltspun CoCu alloys

Magnetic properties and giant magnetoresistance in melt-spun Co-Cu alloys

R. H. Yu,[a] X. X. Zhang, and J. Tejada
Departament de Fisica Fonamental, Facultat de Fisica, Universitat de Barcelona, 08028 Barcelona, Spain

M. Knobel
IFGW, Universidade Estadual de Campinas (Unicamp), C. P. 6165, Campinas 13083-970 S. P., Brazil

P. Tiberto and P. Allia
Dipartimento di Fisica, Politecnico di Torino, I-10129 Torino, Italy

(Received 14 November 1994; accepted for publication 5 March 1995)

Magnetic, structural, and transport properties of as-quenched and annealed $Co_{10}Cu_{90}$ samples have been investigated using x-ray diffraction and a SQUID magnetometer. The largest value of MR change was observed for the as-quenched sample annealed at 450 °C for 30 min. The magnetic and transport properties closely correlate with the microstructure, mainly with Co magnetic particle size and its distribution. For thermal annealing the as-quenched samples below 600 °C, the Co particle diameters increase from 4.0 to 6.0 nm with a magnetoresistance (MR) drop from 33.0% to 5.0% at 10 K. Comparison with the theory indicates that the interfacial electron spin-dependent scattering mechanism correlates with GMR for Co particle diameters up to about 6.0 nm. © *1995 American Institute of Physics.*

I. INTRODUCTION

The discovery of giant magnetoresistance (GMR) and oscillatory interlayer magnetic coupling in Fe/Cr[1–3] multilayers has stimulated considerable interest because of their peculiar magnetic properties and potential use as magnetoresistive devices. The research on GMR and related phenomena was heightened by the recent observation of GMR in magnetic granular systems composed of magnetic clusters embedded in a non-magnetic metallic matrix.[4–6] The present understanding of the GMR in layered structures is based on spin-dependent scattering in magnetic layers as well as at the interfaces between magnetic and non-magnetic layers. Models based on the semiclassical Boltzmann approach[7] and the Kubo formalism[8] have been made to derive the magnetoresistance in the multilayered structures. The spin-dependent scattering of the conduction electrons changes as the magnetic field reorients the magnetic layers. For the current in the plane of the layers (CIP), the mean-free path must exceeds, or at least is comparable to, the thickness of nonmagnetic layers. For the current perpendicular to the plane of the layers (CPP), this length scale does not appear. The magnetoresistance found in magnetic granular systems is closer to CPP-MR of multilayered systems than to the CIP-MR on which most of the current attention is focused. In contrast to layered systems, the magnitude of GMR in granular systems is independent of the direction of the field with respect to the current. Results obtained by Xiao *et al.*[5,9,10] and Berkowitz *et al.*[4] reveal that the GMR both in Co-Ag and Co-Cu systems exceed as much as 25% and depends on the sizes and distributions of the ferromagnetic domains. The measured value of the mean-free path for the Co-Ag system is comparable but larger than the grain size.[9,10] The global magnetization (M) is an appropriate variable to describe the field dependence of GMR. In particular, GMR is approximately proportional to $(M/Ms)^2$, where Ms is the saturation magnetization.

The homogeneous metastable alloys composed of immiscible elements can be prepared by using a variety of nonequilibrium techniques such as evaporation,[11] sputtering,[12] and mechanical alloying,[13] otherwise it is not attainable. The granular magnetic systems are obtained by subsequently annealing the supersaturated solution at elevated temperature. Very recently, the observation of GMR in melt-spun Co_XC_{100-X} alloys ($x \leqslant 30$) has been reported.[6,14–16] In this paper, we confirm this result and present a systematic investigation of the GMR effect in melt-spun $Co_{10}Cu_{90}$ alloy, covering structural, magnetic, and transport properties. Both the magnetic and GMR have been found to depend sensitively on the Co particle size in granular $Co_{10}Cu_{90}$ materials.

II. EXPERIMENT

A rapidly quenched $Cu_{90}Co_{10}$ ribbon was prepared by planar flow casting in a controlled atmosphere on a CuZr drum. The samples were cut from the ribbons 5.0×10^{-3} m in width and 6.0×10^{-5} m in thickness and subsequently subjected to furnace annealing at different temperature in the range of 350–600 °C for 30 min at vacuum of 1.0×10^{-5} Torr, in order to control the size and its distribution of the ferromagnetic Co-rich clusters. After the heat treatment, the oxide layer of the samples was removed using diluted acid solution. Characterization of the samples was carried out on x-ray diffractometer (XRD) with $Cu_{k\alpha1}$ and $Cu_{k\alpha2}$. The magnetic properties were obtained by using a SQUID magnetometer in the temperature range 4.2–300 K. The electrical resistivity $[R(H,T)]$ were measured using a dc four-terminal geometry in a magnetic field up to 50 kOe and with temperature from 10 to 300 K. The magnetic field was applied parallel to the current and to the ribbon surface.

[a]Electronic mail: rhy@hermes.ffn.ub.es

 0021-8979/95/78(1)/392/6/$6.00

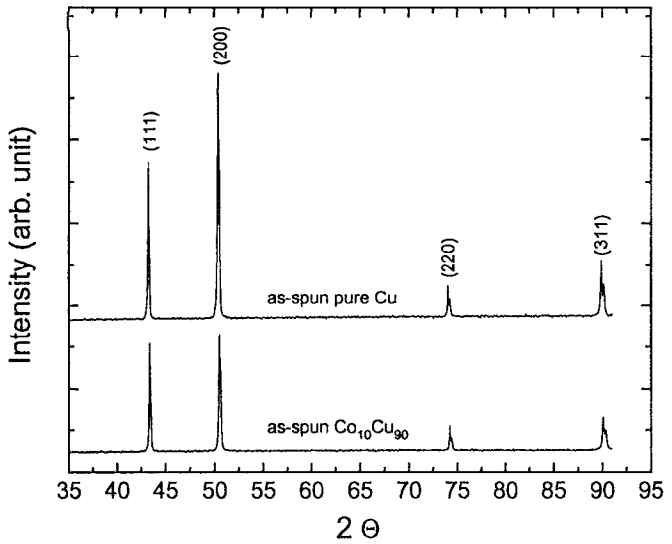

FIG. 1. θ-2θ x-ray spectra for two as-quenched samples of pure Cu and $Co_{10}Cu_{90}$.

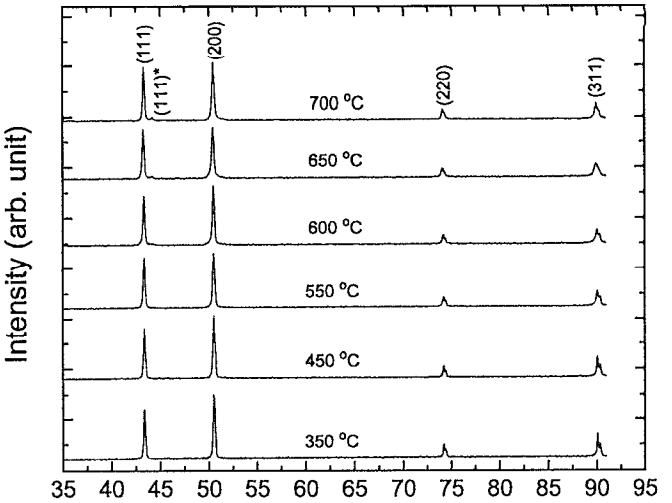

FIG. 2. θ-2θ x-ray spectra for $Co_{10}Cu_{90}$ samples annealed at different temperatures. The (*) denotes the diffraction lines from fcc Co clusters.

III. RESULTS AND DISCUSSION

A. Microstructure evolution and x-ray analysis

The XRD patterns of the as-quenched pure Cu and $Cu_{90}Co_{10}$ ribbons are presented in Fig. 1. Both of the samples show similar and well-resolved diffraction lines at d spacing which are match with that of the face-centered-cubic (fcc) phase. Compared with the XRD pattern of pure Cu, no additional diffraction lines appear, which indicates that the immiscible Cu and Co elements form a homogeneous metastable phase after rapid solidification. The lattice constant for the as-quenched $Cu_{90}Co_{10}$ phase calculated from XRD data is 0.3608 nm, is less than that of pure bulk Cu of 0.3615 nm, but larger than the lattice constant of pure fcc Co of 0.3545 nm. The as-quenched sample is fcc with the lattice spacing intermediate between those of bulk Co and Cu samples, likely due to the substitutional effects of Co atoms. We found that the intensity of (200) line $\mathbf{I}_{(200)}$ is higher than that of (111) line $\mathbf{I}_{(111)}$, indicating the as-quenched ribbons were (200) textured.

The XRD patterns acquired for the samples annealed at different temperatures show the diffraction lines of Co-rich fcc phase which appear at 600 °C and grow in intensity and ultimately become resolved peaks, indicating the presence of a second phase. This is most clearly seen for the sample annealed at 700 °C (see Fig. 2). The lattice constant calculated for this Co second phase in the sample treated at 650 °C for 30 min is 0.3576 nm, higher than the lattice constant of the pure Co phase, owing to the presence of a small amount of Cu atoms in the Co fcc phase. This result indicates that the phase precipitated from the metastable homogeneous matrix is not pure Co clusters but Co-rich second phases. Upon further increasing of the annealing temperature to 700 °C, the lattice constant of Co-rich second phase decreases to a value of 0.3523 nm, which is still higher than that of pure Co. One can imagine the formation of the Co particles as the atom diffusion process which steadily separates the Co atoms from the Cu fcc matrix as the annealing temperature was increased. The diffraction lines corresponding to the Co-rich second phase have not been observed for the samples annealed below the temperature of 500 °C, being due to three reasons:

(1) the coherency at the interfaces of the Co-rich second phase and matrix;
(2) the small size of Co clusters, or merely Co-rich regions formed in the Cu matrix;
(3) the absorption of $Cu_{k\alpha}$ by Co.

As shown in Fig. 1, the grains of the as-quenched $Co_{10}Cu_{90}$ phase are oriented with (200) plane. As the annealing temperature is increased, the intensity of the (200) peak, $\mathbf{I}_{(200)}$, decreases, while the intensity of the (111) peak, $\mathbf{I}_{(111)}$, increased. Here, we introduce the relative intensity $\mathbf{I}_R$ to evaluate the degree of preferred (hkl) orientation obtained by calculating the peak intensities according to the following formula:

$$\mathbf{I}_{R(111)}=[\mathbf{I}_{(111)}/\mathbf{I}_{(200)}]_P/[\mathbf{I}_{(111)}/\mathbf{I}_{(200)}]_S, \quad (1)$$

where the subscripts S and P denote the as-quenched sample and standard bulk Cu sample, respectively. Here, we adopt bulk Cu as reference because of the absence of x-ray data of standard homogeneous metastable Co-Cu samples. $\mathbf{I}_{R(111)}=1$, matching the standard bulk Cu state without texture. $\mathbf{I}_{R(111)}>1$, denoting the preferential (111) orientation, and $\mathbf{I}_{R(111)}<1$, indicating (200) texture. The relation between the annealing temperature and $\mathbf{I}_{R(111)}$ is shown in Fig. 3. As a whole tendency, $\mathbf{I}_{R(111)}$ grows with increasing annealing temperature, but the value of $\mathbf{I}_{R(111)}$ was still lower than 1 even for the sample annealed at 700 °C.

The stable structure of Co at room temperature is a hexagonal-close-packed lattice (hcp). The phase separation temperature for the metastable Co-Cu phase (≈500 °C) is higher than the temperature above which the fcc phase becomes stable in Co (≈425 °C).[17,18] Thus, Co recrystallize in the fcc form at a temperature higher than 425 °C. It is, how-

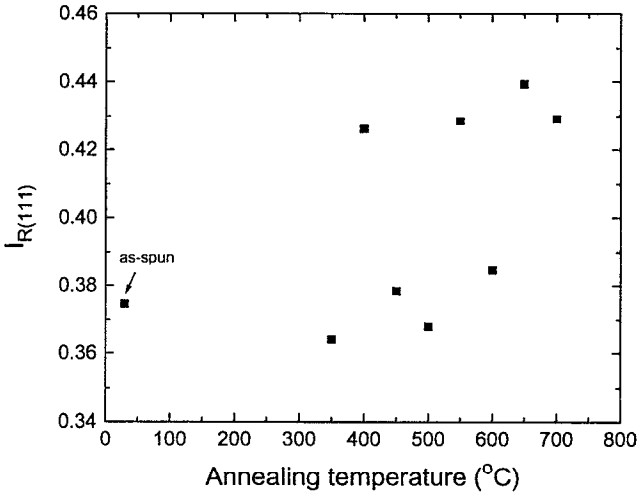

FIG. 3. Relative $I_{R(111)}$ change as the $Co_{10}Cu_{90}$ samples annealed at different temperature.

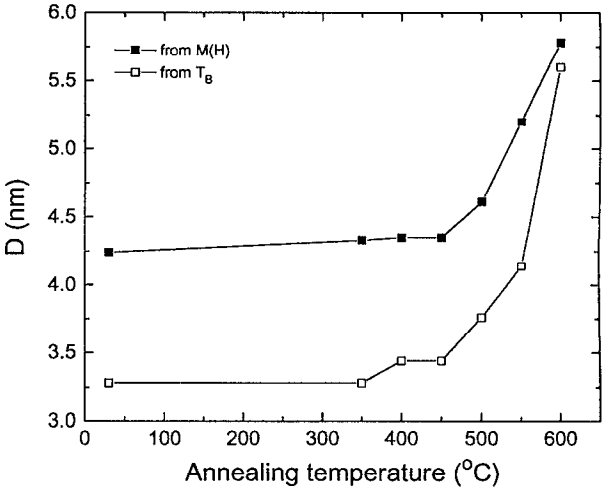

FIG. 5. Co particle diameter as a function of annealing temperature. (○) and (□) represent the values calculated by fitting the Langevin function and blocking temperature of the Co particles.

ever, unexpected that its fcc structure is retained down to room temperature, especially in our experiment where the samples were not quenched, but just cooled down in vacuum after annealing.

B. The magnetic properties and the size of Co particles

As shown in Fig. 1, Fig. 2, and in the previous paper,[19] it is difficult to determine the Co-cluster size by XRD method and TEM because of the high coherency of the Co and Cu lattices and comparatively small lattice mismatch (<2.0%). In addition to microstructural characterizations, however, the magnetic particle size and its distribution can be determined by analyzing the magnetization curves $M(H)$ in superparamagnetic state. Figure 4 shows the $M(H)$ curves of $Co_{10}Cu_{90}$ alloy measured at 295 K, which is much higher than their blocking temperature ($T_B = 10-60$ K). At this temperature, the as-quenched and annealed samples exhibit superparamagnetic behavior. The $M(H)$ of a non-interacting superparamagnetic system with uniform particle size is described by the Langevin equation

$$M(H) = PMsL\left(\frac{\mu H}{k_B T}\right) = PMs\left[\coth\left(\frac{\mu H}{k_B T}\right) - \frac{k_B T}{\mu H}\right], \quad (2)$$

where P is the volume fraction of the magnetic particles, $\mu = MsV$ is the magnetic moment of a single particle with volume V, and H is the external magnetic field. Only using the $M(H)$ data at 295 K, for which the sample is truly in the superparamagnetic regime, a best least-square fit to the magnetization data, can the magnetic moment μ be calculated. Again, using the 0 and 412 K values of the saturation magnetization for pure fcc, 162.5 emu/g (1.435×10^3 emu/cm^3)[23] and 155.2 emu/g (1.371×10^3 emu/cm^3),[24] respectively, we fit the experimental data $M(H)$ at room temperature to Eq. (2) with different sizes of Co particles, and the average Co particle sizes can be determined (see Fig. 5).

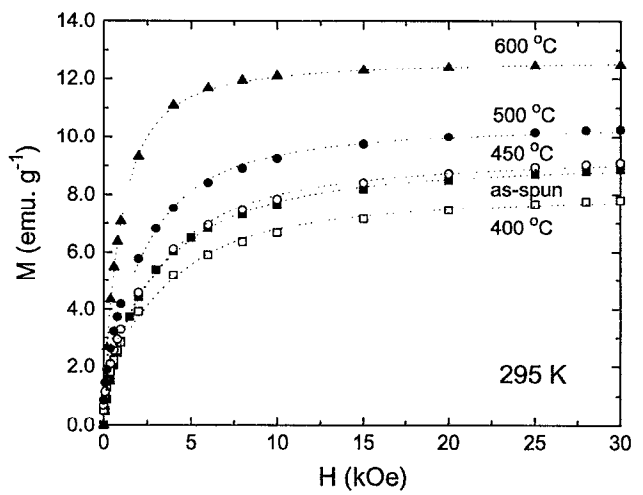

FIG. 4. Room-temperature magnetization curves of $Co_{10}Cu_{90}$ ribbons in as-quenched and annealed states. Symbols (■, etc.) are experimental results and dashed lines are the theoretical values.

Figure 6 shows the magnetization for the samples in both field-cooled (FC) and zero-field cooled (ZFC) states in an applied field of 50 Oe. At the average blocking temperature (T_B), the ZFC and FC curves diverge and the ZFC curve exhibit a peak. The observation of ZFC and FC curves diverging above the peak of ZFC curves [Fig. 6(b)–6(d)] indicates the existence of a broad distribution of the size and shape of the Co magnetic particles. We found that the diverging temperature of ZFC and FC curves increases as the annealing temperature is increased, reflecting, with the growth of the Co magnetic particles.

At sufficiently high temperature, the magnetic anisotropy energy barriers of the single domain particles are overcome by thermal energy, and the superparamagnetism occurs. Superparamagnetic behavior can be observed using an instrument with a characteristic measuring time at the temperature above the blocking temperature (T_B), which is defined as

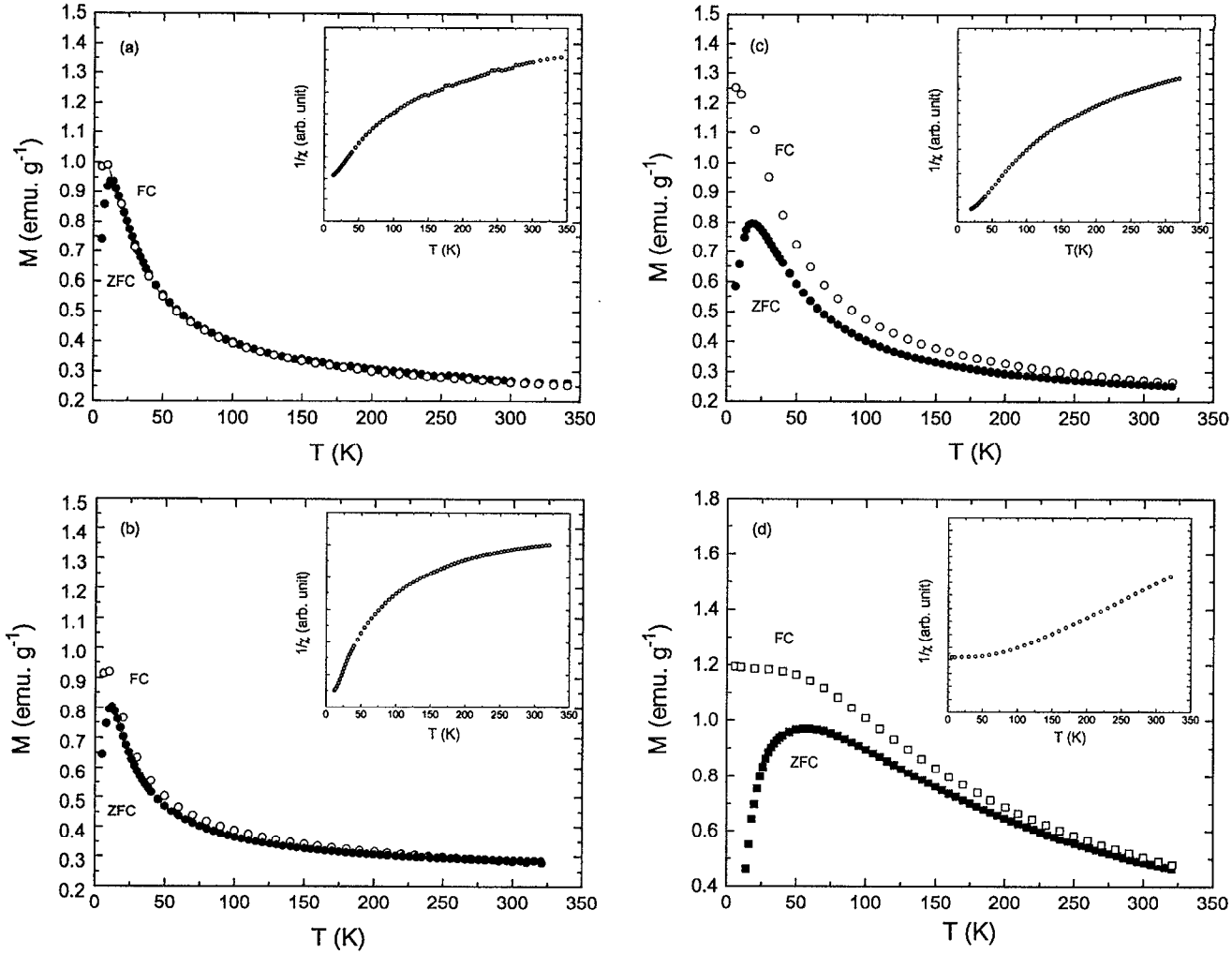

FIG. 6. Magnetization in 50 Oe of the $Co_{10}Cu_{90}$ samples both field cooled (FC) and zero-field cooled (ZFC): (a) as-quenched, (b) annealed at 350 °C, and (c) annealed at 500 °C. The insets show the relation between inverse susceptibility and temperature.

$$T_B=\frac{E_a}{k_B[\ln(\omega_0/\omega)]}=\frac{K\langle V\rangle}{k_B[\ln(\omega_0/\omega)]}=\frac{K\langle V\rangle}{30k_B}, \tag{3}$$

where $E_a=K\langle V\rangle$ is the magnetic anisotropy energy of the particles, K is the total magnetic anisotropy energy per unit volume and $\langle V\rangle$ is the average volume of the Co particle. The factor of 30 represents $\ln(\omega_0/\omega)$, where ω is the inverse of the experimental time constant ($\approx 10^{-2}$ H_Z) and ω_0 an attempt frequency ($\approx 10^{11}$ H_Z). Using the 0 K value of the magnetic anisotropy for fcc Co ($K=-2.7\times10^6$ ergs/cm^3),[25,26] we have calculated the average sizes of the Co particles which are smaller than that calculated by fitting the room temperature $M(H)$ data as shown in Fig. 5. This result may be due to the selected calculating parameters, i.e., larger value of magnetic anisotropy ($K=-2.7\times10^6$ ergs/cm^3) or smaller ω_0 value (10^{11} Hz) which varies in the range 10^9–10^{13} Hz.

The insets of Fig. 6 show the inverse susceptibility ($1/\chi$) and its temperature dependence. The $1/\chi$ data are not linear in T. For typical paramagnetic systems with atomic moments, χ follows the well-known Curie law of $\chi=nP_{\text{eff}}^2\mu_B^2/3k_BT$. Thus, $1/\chi$ will be linear in T. In the case of granular magnetic system at $T>T_B$, χ can be expressed as using Eq. (2), $\chi=PVM_S^2(T)/3k_B$ for $\mu H<k_BT$, and for non-interacting granules. By considering interaction effects, following Chantrell and Wohlfarth,[27] the χ is expressed as $\chi\propto M_S^2(T)/(T-T_0)$. The nonlinearity of $1/\chi$ against T is due to complicated factors, for example, the temperature dependence of $Ms(T)$ and the distribution of Co particle size.

C. Giant magnetoresistance and relation with Co-cluster size

MR was measured at 10 and 295 K in the maximum magnetic fields of 30 and 50 kOe, respectively. The change of resistivity with field was defined as $\Delta R/R=[R(H)-R(H_{\max})]/R(H_{\max})$. The field required to saturate the magnetoresistance is quite high. $\Delta R/R$ vs H is shown in Fig. 7. For the samples as-quenched or annealed at temperatures below 450 °C which are not fully saturated in 30 kOe, otherwise, the samples annealed at relatively high temperatures saturate more quickly. A saturation field of a few kOe were typical for the annealed samples. Figure 7 shows the $\Delta R/R$ in 30 kOe as functions of annealing tem-

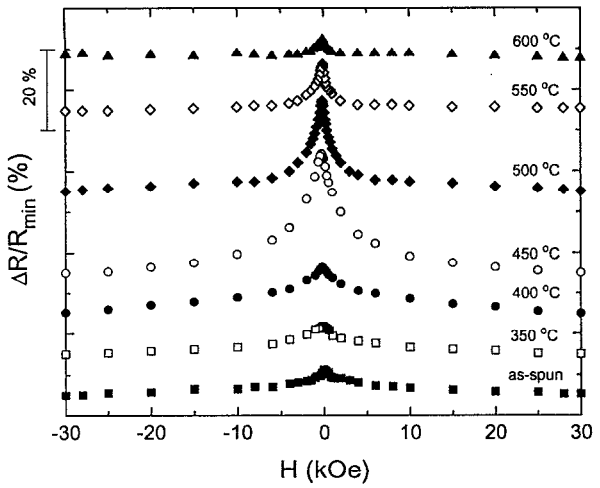

FIG. 7. $\Delta R/R$ vs H for $Co_{10}Cu_{90}$ in as-quenched and annealed states at 10 K.

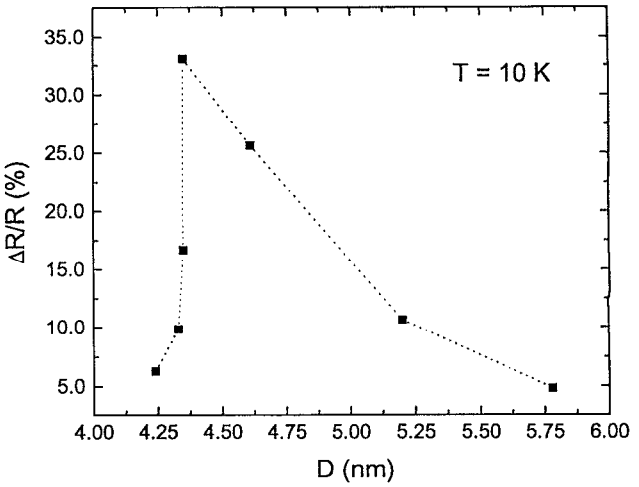

FIG. 8. Dependence of $\Delta R/R$ on average sizes of Co particles.

perature. Here, we focus on the GMR results at low temperature, where phonon and magnon contribution to the resistivity is negligible. The GMR is observed in the granular system formed by aging at high temperature where the granule is well established.

In the as-quenched state the resistance drops only 6.0% up to an external field of 30 kOe. The aging of as-quenched ribbons drastically enhances the GMR as shown in Fig. 7. The maximum in the MR change of 33.0% was achieved for the sample annealed at temperature of 450 °C, which is higher than that reported in the previous papers.[6,14–16] Upon further increase of the annealing temperature, the magnitude of $\Delta R/R$ decreases due to the Co-cluster growth. The apparent dependence of GMR on H is not particularly revealed because GMR is a direct consequence of the field dependence of the global magnetization.[5,20] The highest and the lowest resistances are observed at the original unmagnetized state ($M=0$) and at saturation where all the particles were ferromagnetically aligned ($M=Ms$), respectively. The total resistivity of a granular system can be expressed as[5] $\Delta R/R = -AF(M/Ms)$. The simplest form of $F(x)$ roughly satisfying the GMR data is $F=(M/Ms)^2$, which describes the GMR quite well at low magnetic filed.[5] The crucial factor for the GMR in the granular system is the average $\langle \cos \theta_{ij} \rangle$, where θ_{ij} is the relative angle between the axes of the ferromagnetic entities. The relation $\langle \cos \theta_{ij} \rangle = \langle \cos \theta_j \rangle^2 = (M/Ms)^2$ was observed experimentally. With correlated magnetic axes, a more complicated even function of $(M/Ms)^2$ will be the result. In our case, this relation is in good agreement with experimental results at a low magnetic field (<2 kOe).

The dependence of GMR on annealing conditions is caused by the change in the microstructure of the ribbons upon aging, i.e., the size of Co clusters and its distribution in the Cu matrix. There is small MR change (magnetoresistance $\approx 0.5\%$) in the homogeneous as-deposited sample of $Cu_{80}Co_{20}$ with the magnetic field.[5] In our experiments, however, with the metastable as-quenched sample, a GMR of 6.0% has been observed at 10 K. Based on the magnetic measurements, we assume that some magnetic domains with a relatively less Co atom concentration were formed during the rapid solidification. Annealing the as-quenched ribbons at temperatures below 450 °C, Co clusters of relatively small size were mainly nucleated in Co-rich regions. In the view of kinetics, the formation process of the Co clusters is dominated by nucleation. Annealing the as-quenched ribbons at 450 °C is appropriate for obtaining higher GMR. At this temperature (450 °C), the fine Co particles were fully nucleated before growth. The drop of GMR for the specimen annealed at high temperatures is ascribed to the fractional reduction of Co atoms located at the cluster-matrix interfaces due to the growth of Co particles.

Figure 8 shows the relation between the MR value and Co particle size obtained by fitting the $M(H)$ data at room temperature. The maximum value of MR occurs at a diameter of about 4.4 nm. As shown in Figs. 5 and 6, at 10 K the number of blocked Co particles decreases as the particle size is decreased; small magnetic particles will subject to thermally activated magnetization reversal, i.e., superparamagnetism; and therefore, the ratios of spin-dependent to spin-independent scattering potentials in the magnetic particles and at the cluster-matrix interfaces may be sharply reduced.[28,29] For the fixed magnetic field (30 kOe) and temperature (10 K), the $R(H)$ for ultrafine granules is very difficult to saturate as shown in Fig. 7; thus, the magnitude of $\Delta R/R$ decrease with decreasing Co particle size for the diameter $D<4.4$ nm, which is similar to that the magnitude of $\Delta R/R$ decreases with increasing temperature. For the Co particles with a diameter $D>4.4$ nm, the decrease of the magnitude of $\Delta R/R$ with increasing particle size may also be due to additional factors[4] besides the reduction of the Co particle surface to volume ratios. First, the Co particles will become larger than the mean-free path within the particles. Second, when the particles are no longer single domain, the interaction of the conduction electron spins with varying magnetization distribution in the particles produces a state in which the conduction electron channels are mixed.

Most models of GMR are based on the fundamental assumption that the current is carried in two independent conduction channels related to the spin-up and spin-down electrons. The magnetic field dependence of the resistivity is attributed to spin-dependent scattering occurring within the ferromagnetic clusters and at the interfaces between magnetic and non-magnetic entities. Our experiments confirm (Fig. 8) that the interfacial spin-dependent scattering is the dominant mechanism for GMR in granular Co-Cu systems as suggested in the previous paper.[19] According to the phenomenological models,[28,29] the change of MR should scale approximately as the magnetic particle surface to volume ratio if the interfacial spin-dependent scattering is the dominant mechanism for GMR. Alternatively, if the spin-independent volume scattering dominates, then the MR change depends weakly on the magnetic particle sizes.

We should also indicate that the GMR in the granular alloys does not only depend on the average size of ferromagnetic particles embedded in the matrix, but to a large extent on the distribution of the particle size. Such results will be published elsewhere.

IV. CONCLUSIONS

We have investigated the structural, magnetic, and transport properties of as-quenched $Co_{10}Cu_{90}$ granular alloys. The results by calculating the magnetic data confirmed that these samples consist of ultrafine Co magnetic particles dispersed in the samples with size distributions. The value of $M(H)$ and MR have been found to depend sensitively on Co particle sizes, as well as the distribution of Co magnetic particles in the Cu matrix. The maximum change of MR, about 30% at 10 K for a magnetic field of 30 kOe, occurs at the Co particle diameter of about 4.4 nm. As the Co particle diameter is larger than 4.4 nm, the value of MR is drastically decreased.

[1] M. N. Baibich, J. M. Broto, A. Fert, F. Nguyen van Dau, F. Petroff, P. Etienne, G. Creuzet, A. Friederich, and J. Chazeles, *Phys. Rev. Lett.* **61**, 2472 (1988).
[2] G. Binasch, P. Grunberg, F. Saurenbach, and W. Zinn, Phys. Rev. B **39**, 4828 (1989).
[3] S. P. Parkin, N. More, and K. P. Roche, Phys. Rev. Lett. **64**, 2304 (1990).
[4] A. E. Berkowitz, J. R. Mitchell, M. J. Carey, A. P. Young, S. Zhang, F. E. Spada, F. T. Parker, A. Hutten, and G. Thomas, Phys. Rev. Lett. **68**, 3745 (1992).
[5] J. Q. Xiao, J. S. Jiang, and C. L. Chien, Phys. Rev. Lett. **68**, 3749 (1992).
[6] J. Wecker, R. von Helmolt, L. Schultz, and K. Samwer, Appl. Phys. Lett. **62**, 1985 (1993).
[7] R. E. Camley and J. Barnas, Phys. Rev. Lett. **63**, 664 (1989).
[8] P. M. Levy, S. Zhang, and A. Fert, Phys. Rev. Lett. **65**, 1643 (1990).
[9] J. Q. Xiao, J. S. Jiang, and C. L. Chien, Phys. Rev. B **46**, 9266 (1992).
[10] P. Xiong, G. Xiao, J. Q. Wang, J. Q. Xiao, J. S. Jiang, and C. L. Chien, Phys. Rev. Lett. **69**, 3220 (1992).
[11] E. Kneller, J. Appl. Phys. **33**, 1355 (1963).
[12] C. L. Chien, S. H. Liou, G. Xiao, and M. A. Gatzke, Mater. Res. Soc. Symp. **80**, 395 (1993).
[13] J. G. Cabañas-Moreno, V. M. Lopez, H. A. Calderon, and R. Angeles, Scripta Met. **28**, 645 (1993).
[14] B. Dieny, A. Chamberod, C. Cowache, J. B. Genin, S. R. Teixeira, R. Ferre, and B. Barbara, J. Magn. Magn. Mater. **126**, 433 (1993).
[15] H. Takeda, N. Kataoka, K. Fukamichi, and Y. Shimada, Jpn. J. Appl. Phys. **33**, L102 (1994).
[16] N. Kataoka, H. Endo, K. Fukamichi, and Y. Shimada, Jpn. J. Appl. Phys. **32**, 1969 (1993).
[17] T. Nishizawa and K. Ishida, Bull. Alloy Phase Diagram **5**, 161 (1984).
[18] J. R. Chidress and C. L. Chien, J. Appl. Phys. **70**, 5885 (1991).
[19] T. A. Rabedeau, M. F. Toney, R. F. Marks, S. S. P. Parkin, R. F. C. Farrow, and G. R. Harp, Phys. Rev. B **48**, 16810 (1993).
[20] G. Xiao and C. L. Chien, J. Appl. Phys. **61**, 3308 (1987).
[21] C. L. Chien, J. Q. Xiao, and J. S. Jiang, J. Appl. Phys. **73**, 5309 (1993).
[22] J. Q. Wang and G. Xiao, Phys. Rev. B **49**, 3982 (1994).
[23] B. D. Cullity, *Introduction to Magnetic Materials* (Addison-Wesley, Reading, MA, 1972).
[24] J. Crangle, Philos. Mag. **46**, 499 (1955).
[25] W. D. Doyle and P. J. Flanders, International Conference on Magnetism, Nottingham, 1964, p. 751.
[26] W. A. Sucksmith and J. E. Thompson, Proc. R. Soc. (London) A **22**, 362 (1954).
[27] R. W. Chantrell and E. P. Wohlforth, J. Magn. Magn. Mater. **40**, 1 (1983).
[28] S. Zhang, Appl. Phys. Lett. **61**, 1855 (1992).
[29] S. Zhang and P. M. Levy, J. Appl. Phys. **73**, 5315 (1993).